Mechanistic insights into the sediment accumulation and fractionation of PAHs: Role of sedimentary organic carbon and an assessment of environmental implications

Weijie Liu [a, c]; Xinli Xing [a, b]*; Xingchen Liu [c]; Andrew Sweetman [c]; Kevin C. Jones [c]; Gaigai He [a]; Shibin Qin [d]; Li Liu [e]; Peng Li [e]; Xiaoshui Li [b], Shihua Qi [a, b];

a, School of Environmental Studies, China University of Geosciences, Wuhan 430074, China

b, State Key Laboratory of Geomicrobiology and Environmental Changes, China University of Geosciences, Wuhan 430074, China

c, Lancaster Environment Centre, Lancaster University, Lancaster, LA1 4YQ, UK

d, Institute of Eco-Environmental Research, Guangxi Academy of Sciences, Nanning, 530007, China

e, Hubei Geological Bureau, Wuhan 430034, China

* To whom correspondence should be addressed Email: xlxing@cug.edu.cn ;

Abstract:

Increasing anthropogenic activities and carbon aging processes present a significant global concern in understanding the accumulation mechanisms of polycyclic aromatic hydrocarbons (PAHs) in sediments, especially regarding the overlooked role of nonextractable residues (NERs). Here we investigated the accumulation patterns of three PAHs fractions (bioavailable-BPAHs, extractable -EPAHs, and NERs), hydrodynamic conditions and organic matter sources of sediment across different types lakes. This study reveals a previously unrecognized potential relationship among anthropogenic factors, including hydrodynamic condition, sedimentary organic carbon (SOC) profiles, and PAH fractions based on the mantel test and structural equation model (SEM). A significant feature influencing the occurrence of EPAHs and NERs was attributed to SOC fractions, especially for sedimentary labile (LOC) and recalcitrant organic carbon

(ROC) pools. LOC mainly controlled the EPAH distributions, while ROC may further accelerate the sedimentary accumulation of NERs. The potential accumulation mechanism affecting the fractionation of PAHs was further captured by quantitative structure activity relationship (QSAR) modelling. A strong relationship between less hydrophobic PAHs and the proportion of EPAHs was attributed to molecular reactivity and mobility based on high Egap, increased entropy, and van der Waals interactions. However, the formation of NERs was primarily driven by molecular polarity (μ, α) and electrophilic potential (qC^+). The inclusion of BPAHs into PAH-based risk calculations and subsequent sediment management strategies is recommended, improving our understanding of the environment significance of the three PAHs fractions. Overall, these findings provided a mechanistic insight into the coupling between sedimentary carbon composition and the fate of PAHs.

Key words: Polycyclic aromatic hydrocarbons; NERs fraction; Sedimentary organic carbon fractions; Accumulation mechanisms; Environmental risk assessment;

1. Introduction

Polycyclic aromatic hydrocarbons (PAHs) are environmental contaminants of concern because of their inherent toxicity, mutagenic and carcinogenic properties, and their resistance to microbial degradation (Cao et al., 2025; Zeng et al., 2023). Recognized as priority pollutants by the US Environmental Protection Agency (USEPA), Europe, and China, PAHs enter the environment (aquatic and soil environment) through both natural and anthropogenic sources, including volcanic activity, fossil fuel combustion, forest fires, vehicle emissions, wastewater within industrial processes (Gholami et al., 2024; Gómez-Avila et al., 2025). According to the Cao et al. (2025), relatively high levels of PAHs (ranging from 161.17 $ng \cdot L^{-1}$ to 1185.59 $ng \cdot L^{-1}$) were foubd compared to others microorganic pollutants in surface water across China. Further, PAHs adsorb strongly onto

sediment particles due to their high hydrophobicity and chemical stability, thereby enabling their long-term persistence in aquatic environment. Sediments can act as secondary sources of PAHs when environmental disturbances (such as flooding, hydraulic engineering, and urban runoff) change sedimentary conditions, resulting in the remobilization of sorbed pollutants, thereby reintroducing risks to aquatic ecosystems (Maletic et al., 2019). Consequently, understanding their fate in sediment is critical to manage their presence.

Previous studies have emphasized the extractable fraction of PAHs in sediments as the main reservoir, while neglecting the significance and formation of non-extractable residues (NERs) (Ma et al., 2025; Zhu et al., 2023). The formation mechanisms of NERs include physical encapsulation (including entrapment and adsorption), covalent bonding (e.g., ester, ether, amide, and carbon-carbon linkages), and association with microbial biomass, which is regarded as a natural detoxification pathway (Gevao et al., 2000; Kästner et al., 2014). However, NERs may still pose environmental risks if their reversible components (such as the physical encapsulation part and ester-bound formation) are remobilized into the extractable fraction under the alterations to sediment conditions (Wu et al., 2024). For example, case studies have proven that 2-60% NERs may become remobilized along with changes to sediment physicochemical properties, redox condition, and microbial activity (Liu et al., 2013; Schäffer et al., 2018). Meanwhile, the NERs formation in sediment may change the component profile of PAHs, particularly their ring-number distribution, thereby affecting their toxicological profile (Qin et al., 2025). Therefore, the true PAHs inventory in sediment should not be underestimated.

The accumulation of PAHs in sediment is primarily controlled by sediment organic matter, such as humification process enhancing the adsorption of naphthalene (Liu et al., 2025). Increasing sediment organic carbon (SOC) in sediments has been shown to significantly decrease PAH bioaccumulation (Skic et al., 2023). Generally, easily oxidizable organic carbon (EOC) (such as fulvic acid and humic acid) can enhance the

bioavailability of PAHs, while the adsorption of PAHs onto sediment-bound humin prevents their mobility (Gholami et al., 2024). Consequently, SOC is commonly divided into labile (LOC) and recalcitrant organic carbon (ROC) pools to capture differences in their decomposition rates, stability, and turnover, allowing for a more accurate characterization of SOC composition and behavior (Lian et al., 2018). LOC pools, including EOC, light fraction organic carbon (LFOC) and microbial biomass carbon (MBC), function as an immediately accessible nutrient source for aquatic primary producers and microorganisms, characterized by its high biodegradability and rapid turnover rate (Ma et al., 2020). A higher proportion of ROC in sediment is usually beneficial for the stabilization and storage of SOC as it primarily consists of refractory compounds enriched in aromatic hydrocarbons and alkanes, including lipids, cellulose, and lignin (Serrano et al., 2020; Trevathan-Tackett et al., 2017). Hydrological processes and lake eutrophication can usually regulate carbon fractions and PAH burial (Ji et al., 2024; Ya et al., 2022). Physical disturbances promote the degradation of ROC in sediment (Arzayus and Canuel, 2005), and hydrological processes have been shown to markedly affect the distribution of PAHs in the Danjiangkou Reservoir (Dong et al., 2025). However, information establishing PAHs fractionation, SOC profiles, and hydrological characteristics of different types of lakes are limited.

Overall, we hypothesize that the extractable fraction and NERs of PAHs are mainly regulated by hydrological processes and SOC profiles in sediment. Herein, we have selected five different lake types to investigate the fractionation of PAHs in sediment. The objectives of current study were (1) to characterize PAHs fractionation patterns, hydrodynamic conditions, and sediment organic matter sources; (2) to investigate the potential pathways affecting the PAHs fractionation and uncover the relationships among anthropogenic disturbances, hydrodynamic conditions, SOC profiles, and PAH fractions; (3) to explore the potential mechanisms underlying accumulation of different PAHs fractionation and assess their environment implications.

2. Materials and methods

2.1 Study area and sampling

Wuhan, often referred to as the "City of a Hundred Lakes", has evolved in close conjunction with its fluvial and lacustrine systems, whereby changes in lake morphology have played a pivotal role in shaping its urban form (Li et al., 2025). Since the early twentieth century, lake dynamics within the city's core have been particularly pronounced, coinciding with the most accelerated phase of urban expansion (Shi et al., 2022). From September 2020 to July 2022, 5 lakes were selected based on population and economic development levels characterizing the intensity of anthropogenic disturbances. Within Wuhan's urban lacustrine network, Tangxun Lake (TXH) stands as China's largest urban lake (Shi et al., 2022), and Moshui Lake (MS) and Longyang Lake (LY) function as the primary gateways in the Wuhan's "Six Lakes Connectivity" initiative (Zhang et al., 2025). For rural lakes, Chenhu Lake (CH) is recognized as a wetland of international importance and has been designated as a provincial-level nature reserve (Xing et al., 2023), Liangzi Lake (LZH) receives the highest ecological protection due to its important ecosystem service values (Niu et al., 2023). For this study, 74 sampling sites were selected within different lake types using a stainless-steel grab sampler (LY: 11 sites, MS: 16 sites, TXH: 22 sites, CH: 13 sites, and LZH: 12 sites). The sediment samples were promptly wrapped in aluminum foil and stored in clean polyethylene bags to preserve their integrity. All sediment samples were air-dried and sieved through 0.15 mm pores, then stored at -20 °C until geochemical analysis. The information on sampling sites within different types was shown in Fig S1.

2.2 Chemical analysis

15 PAH congeners were selected for this study with their physicochemical parameters shown in Table S1. The analytical procedure for the target compounds was conducted in accordance with our previous studies

using the synthesized magnetic adsorbents (Fe_3O_4@PDA, Fe_3O_4@PDA@PDVB, and Fe_3O_4@PCD) (Qin et al., 2024; 2021). The three PAHs fractions were sequentially extracted, including the bioavailable (BPAHs), extractable (EPAHs), and NERs. Briefly, sediment (1.00g) was placed into a vial containing 30mg Fe_3O_4@PCD and 15mL mixture (NaN_3: $1 g \cdot L^{-1}$ and HPCD: $10 g \cdot L^{-1}$). The mixture vial was shaken at 150rpm and 25°C for 24 hours. After extraction, the magnetic adsorbent was retrieved by magnetic separation and the bound PAHs (BPAHs) subsequently desorbed for analysis according to Qin et al. (2021).

The residual sediment was immediately mixed with 12mL mixture of Acetone (Ace): n-hexane (Hex) (1:1, v: v) for EPAHs extraction. The mixed solution was extracted using 15min ultrasonication, followed by centrifugation. The extraction process was repeated three times by adding fresh solvent. The residual sediment was subsequently rinsed twice (10 s vortex) with the same extraction solvent, and all supernatants plus washings were combined to yield the EPAH fraction. After this the extracts were purified and concentrated.

Following extraction the washed sediment residue was derivatized by silylation reaction with 2 mL dimethyl sulfoxide, 200 µL chlorotrimethylsilane, and 10 µL pyridine at 25 °C and 120 rpm for 12 h. After the silation reaction, target compounds were captured by polydivinylbenzene-coated magnetic polydopamine particles, and the residual sediment extracted twice with 12 mL Hex: Ace (1:1 v/v). The combined mixture with supernatants and extract were defined as the F1 fraction. The remaining sediment was then digested with 10 mL of 6 M hydrofluoric/hydrochloric acid at 60 °C and 120 rpm for 4 h. Following acid removal and drying, the residues were again twice extracted with 12 mL Hex: Ace (1:1 v/v) to collect the F2 fraction. The NERs were quantified as the sum of F1 and F2. Detailed information about the cleanup procedures and reagent specifications are provided in Text S1 and S2. The three PAHs fractions were quantified by gas chromatograph-mass spectrometry (6890N-5975C, GC-MS, Agilent), with a chromatographic column of quartz capillary (DB-5MS, 30×0.25mm×0.25µm). 1000 ng of hexamethylbenzene (HMB; Dr. Ehrensorfer,

Germany) was spiked into the final extract as an internal standard. Detailed purification and chromatographic conditions are presented in Text S3.

2.3 Sediment characterization

TOC and total nitrogen (TN) of the dried sediment samples were determined using a vario TOC cube analyzer (Elementar, Germany). In this study, TOC was partitioned into LOC and ROC fractions. The ROC pool was measured by acid hydrolysis (Dodla et al., 2012; Lian et al., 2018). In brief, sediment was digested with 6 M HCl at a 1:10 (w/v) ratio for 16h. The mixture was subsequently centrifuged and the supernatant discarded. The remaining sediment, defined as the ROC fraction, was washed with deionized water and naturally air dried. Then the sediment residue (ROC) was determined by a vario TOC cube analyzer. LOC was calculated by subtracting ROC from TOC. The stable carbon isotope content for $\delta^{13}C$ was measured by isotope-ratio mass spectrometry (MAT 253, Thermo scientific, Germany) (Xing et al., 2023). Grain size distribution of sediment, representing the hydrodynamic conditions, was determined using a Mastersizer 3000 (Malvern Instruments, UK), as shown in our previous study (Cheng et al., 2021). More information about sediment grain size is presented in Text S4. The carbon stability index (CSI) is defined as the ratio of ROC and TOC according to an earlier study (Lian et al., 2018). Carbon use efficiency from stoichiometry theory (CUEST) was used to get determine the sediment CUE (Sinsabaugh et al., 2016).

2.4 Data processing and statistical analyses

The cluster analysis, random forest model, mantel test, and structural equation model (SEM) were performed using R studio 2024 (Posit, USA) (R package “EMMAgeo”, “forecast”, “randomForest”, “pls”, “piecewiseSEM”, “linkET”, and “lme4”). The stable isotope-based multivariate mixture model was conducted to determine the sedimentary OM sources and the remaining information is presented in Text S5. The sediment PAH accumulation was determined by both sediment characteristics and PAH molecular properties (Liu et al.,

2023a). According to Marquès et al. (2017), PAH molecular structures were optimized using Gaussian 09W at the B3LYP/6-311G** level. 13 PAH molecular descriptors were extracted (Li et al., 2024) (Table S2). A quantitative structure - activity relationship (QSAR) model of PAH chemical structural parameters and the PAHs fractions was constructed by using R studio with random forest model and partial least squares model. The optimal solution of the selected model was confirmed by the coefficient of determination (R^2) between predicted value and actual value and root mean square error (*RMSE*). In this study, the incremental lifetime carcinogenic risk (ILRs) of seven carcinogenic PAHs was calculated to assess the environmental significance of three PAHs fractions. Other information about ILRs were listed in Text S6 and Table S3. Additional statistical analyses and visualization were conducted using OriginPro 2024 (OriginLab Corp., USA).

2.5 Quality assurance and control

Quality assurance measures included sample and procedural blanks, reagent blanks, and triplicate analyses were undertaken during the chemical analysis. The average recoveries (±SD) of the four deuterated internal standards were 91 ± 11% (Acenaphthene-d_{10}), 110 ± 9% (Phenanthrene-d_{10}), 107 ± 13% (Chrysene-d_{12}) and 91 ± 12% (Perylene-d_{10}). Relative standard deviations for all replicates remained below 5% (TOC, ROC, and TN), with isotopic precision ($\delta^{13}C$) better than 0.3% and grain-size reproducibility within 1%.

3. Result and Discussion

3.1 PAHs fractionation patterns

The fractionation pattern, spatial distribution, and compositional profiles of PAHs are shown in Fig. 1 and Table S4. PAHs across the three fractions ranged from 51.12 to 1158.7 $ng \cdot g^{-1}$ for BPAHs, 95.56 to 9743.04 $ng \cdot g^{-1}$ for EPAHs, 175.78 to 2531.27 $ng \cdot g^{-1}$ for NERs, with average concentrations of 270.86 $ng \cdot g^{-1}$ for BPAHs, 1238.46 $ng \cdot g^{-1}$ for EPAHs, 432.08 $ng \cdot g^{-1}$ for NERs, respectively. Phe, Fla, Pyr were consistently dominant

across the different PAH fractions, making a significant contribution to the overall PAH burden (Fig. S2). For BPAHs and EPAHs, the average concentration in rural-type lakes (CH and LZH) was significantly lower than that in urban lake (LY, MS, and TXH) sediments (Table S4), which is associated with anthropogenic activities, including high population density, advanced transportation networks, and developed industrial zones (Luo et al., 2025). Sediments have become micro-pollutant sinks due to their high absorption capacity under low energy conditions (Liao et al., 2025). Despite the lower proportion of NERs concentrations present in MS and TXH, the contribution of NERs in rural-type lakes should not be underestimated. Overlooking NERs fraction may potentially affect accurately determining source apportionment and the development of effective pollution control strategies (Qin et al., 2024). Meanwhile, the pronounced spatial variability (>50%, in Table S5) of BPAHs and EPAHs, rather than NERs (<50%), highlighted the influence of point-source discharges in urban lakes (Luo et al., 2025). These findings suggest that PAHs tend to exist in bioavailable and extractable fractions when they were directly discharged into lake systems, whereas the formation of NERs was generally associated with long-term aging and sequestration processes (Yun et al., 2024).

Similar geographical patterns for the three PAHs fractions were observed, where urban lakes exhibited markedly higher PAHs levels (Fig. 1f, 1g, and 1h), reflecting that PAHs fractionation profiles are generally influenced by anthropogenic activities. Meanwhile, the relatively lower loadings and spatial heterogeneity (<20%) of BPAHs and EPAHs in rural lakes sediments suggested the weaker anthropogenic inputs (Xing et al., 2023). The data suggests that the EPAHs concentrations were significantly lower than the NERs in CH (p<0.001), while others lakes sediment showed diverging patterns, with EPAHs being the dominant fraction. Notably, CH, which is a nationally protected wetland, has likely minimized external PAH inputs under strict environmental regulations (Ma et al., 2022). Consequently, the sequestration of historically deposited PAHs may have caused a higher proportion of NERs in CH (Liu et al., 2023b). These behaviors underscored the

importance of considering both stable and labile PAH fractions and the complexity of PAH fractionation equilibria in aquatic environments when assessing sediment-associated PAHs risks.

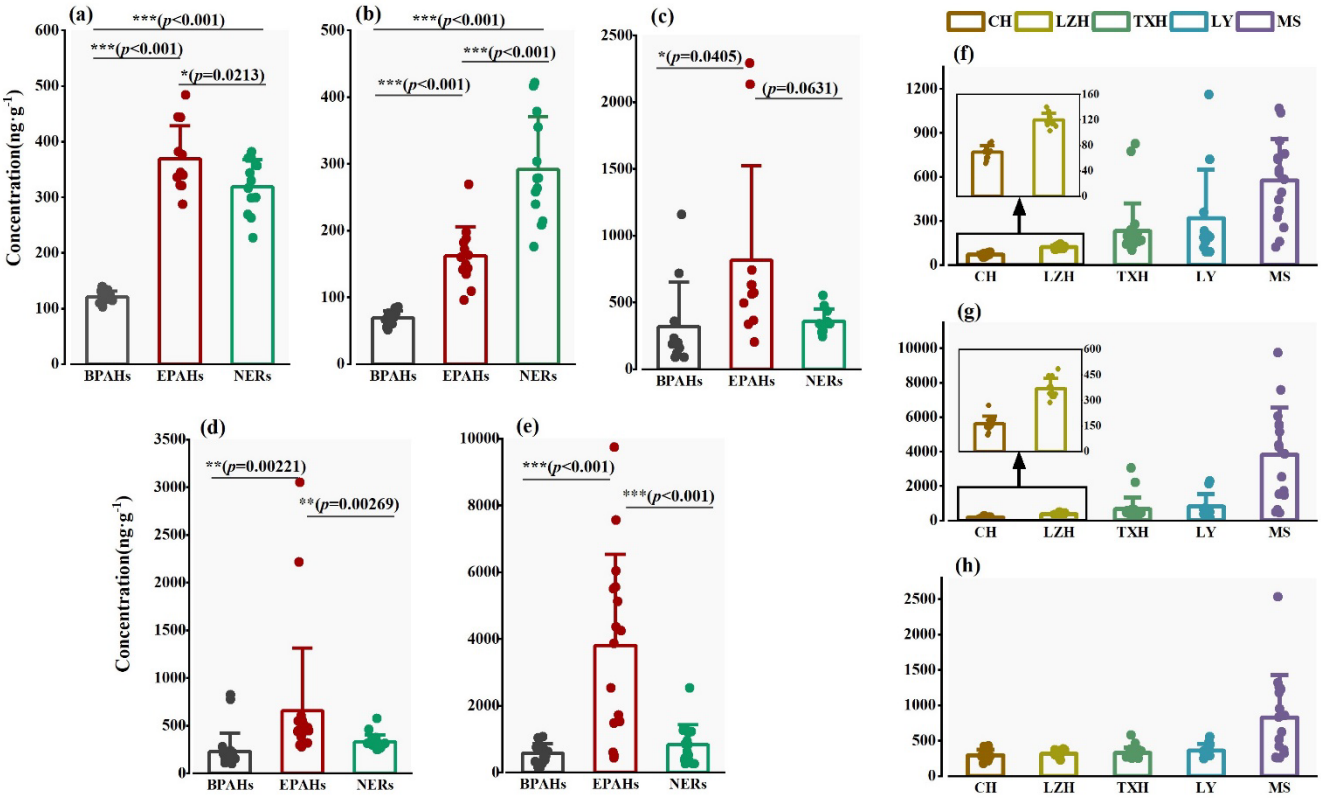

Fig. 1. Statistical differences and geographical features of three PAHs fractions in sediments from five lakes: (a) LZH, (b) CH, (c) LY, (d) TXH, and (e) MS; (f) BPAHs, (g) EPAHs, and (h) NERs.

The binding effect showing the relationship between the hydrophobicity of PAH congeners (log Kow) and EPAHs and NERs is presented in Fig. 2. Specifically, the percentage of EPAHs exhibited a strong positive correlation with hydrophobicity of PAH (R^2=0.718, p<0.0001), whereas a significant negative correlation is presented by the proportion of NERs (R^2=0.869, p<0.0001). The binding effect indicates a mechanistic shift in PAHs - sediment interactions, from PAHs being predominantly associated with weakly bound, rapidly desorption sites to being strongly bound at high-affinity sorption sites (Kästner et al., 2014; Ya et al., 2022). This shift may be attributed to the increased extractability of PAH by organic solvents with the increase of hydrophobicity, whereas PAH with lower hydrophobicity were more likely to penetrate into the microporous structures of OM or bind to high-energy sorption sites embedded within black carbon or humic substance

matrices (Wei et al., 2023; Wei et al., 2024). These results highlighted the change in the sorption-desorption dynamics driven by increasing molecular hydrophobicity and the matrix binding heterogeneity. Meanwhile, it was necessary to further elucidate the underlying mechanisms of the threshold effect.

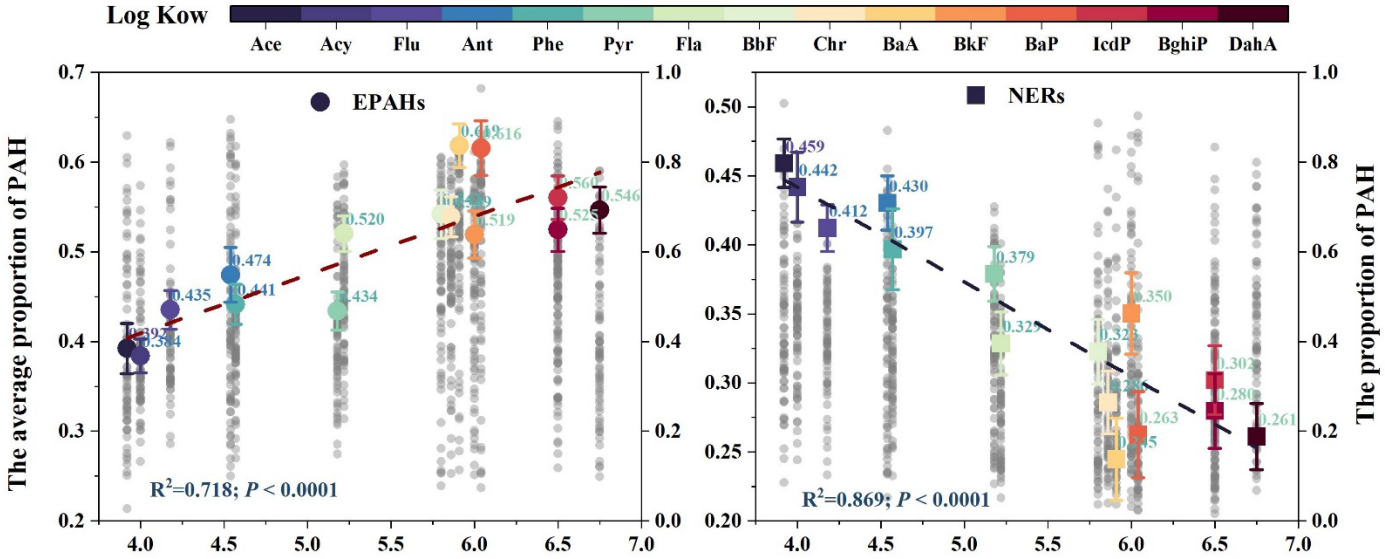

Fig. 2. The relationship between log Kow and percentage of EPAHs and NERs

3.2 Sediment provenance

3.2.1 Hydrodynamic conditions

The grain size distribution was predominantly composed of clay, silt, and sand, as shown in Fig S3 and Table S6, with silt fractions mainly consisting of very fine (VF), fine (FS), medium (MS), and coarse silt (CS) (Hasan et al., 2023; Khan, 2024). The sedimentary patterns revealed the dominance of silty sediments across the different lakes. The skewness and kurtosis of the sediment data, and the significant difference between urban and rural lakes, is presented in Fig S4. It indicates the predominance of fine particles with well-sorted characteristics under stable hydrodynamic conditions in rural lakes (Xing et al., 2023), whereas urban lakes sediment was possibly characterized by the intermittent sediment transport processes or anthropogenic disturbances (Zhang et al., 2025). A clear negative correlation between very fine silt (4-8 μm) and coarse silt

(31-64 μm) was observed across all lake sediment samples (Fig S5), indicating hydrodynamic sorting processes within the lake system. Cluster 1 was characterized by high fine silt and low coarse particles, primarily associated with the CH sediment, indicative of low energy depositional conditions. In contrast, Cluster 2 represented high energy conditions with coarse particle dominance, mainly associated with TXH and MS sediment. Cluster 3 exhibited intermediate properties, suggesting the mixed sedimentation dynamics condition (Eltijani et al., 2022). These patterns implied spatial heterogeneity in sediment stability and could potentially distinct pollutant retention mechanisms across different lakes (Bábek et al., 2020).

3.2.2 Sedimentary organic matter sources

As shown in Table S7, the LOC, ROC, TN, $\delta^{13}C$ of TOC, and C/N profiles ranged from 0.29 to 4.49%, 0.069 to 0.54%, 0.12 to 0.21%, -29.66 to -23.41‰, and 3.99 to 60.38, respectively, with their corresponding average level as 2.09 ± 0.95%, 0.28 ± 0.13%, 0.10 ± 0.026%, -25.89 ± 1.35‰, and 23.08 ± 10.61, respectively. Notably, LOC values in rural lake sediments (CH: 1.23 ± 0.44 %, LZH: 1.43 ± 0.59 %) were significantly lower than those observed in urban lake sediments (LY: 2.35 ± 0.73 %, TXH: 1.93 ± 0.72 %, MS: 3.17 ± 0.85 %), whereas ROC concentrations exhibited an opposing trend, with higher levels observed in rural lake sediments (as shown in Table S). Generally, LOC fractions in sediments can be attributed to stormwater runoff and algal production, which are rapidly mineralized in aquatic environments (Zhang et al., 2023). In contrast, higher ROC values in sediments are primarily associated with terrestrial-derived humic substances and autochthonous phytoplankton, which are structurally complex and recalcitrant to microbial degradation (Guo et al., 2025a). According to $\delta^{13}C$ data for the organic carbon pools and C/N ratio, OM sources across the different lake sediments were apportioned based on stable isotope multivariate mixture models (Fig 3). As described by previous studies, four end-members of $\delta^{13}C$ and C/N were sequentially collected in Fig S6,

including atmospheric deposition, sewage organic input, phytoplankton, and soil erosion. Results suggest that a higher contribution from atmospheric deposition in urban lake sediments was closely linked to their high LOC loading, which could be caused by the high concentration of anthropogenic aerosols derived from vehicular emissions, industrial activities, and domestic sources (Lian et al., 2018; Lu et al., 2023). This suggestion is corroborated by the positive correlations (Fig S7) between LOC and the proportion of organic matter derived from atmospheric deposition. However, the elevated accumulation from soil erosion and autochthonous phytoplankton in rural lakes (CH and LZH) could be primarily responsible for the accumulation of ROC in sediments, which was further supported by the positive correlations between ROC and the contributions from soil erosion and phytoplankton (Fig S7). A potential explanation is that the undisturbed catchments with natural vegetation promoted the input of lignin- and humic-rich SOM, and the favorable conditions of rural lakes supported the phytoplankton production, contributing notably to the sedimentary OM pool (Lu et al., 2023).

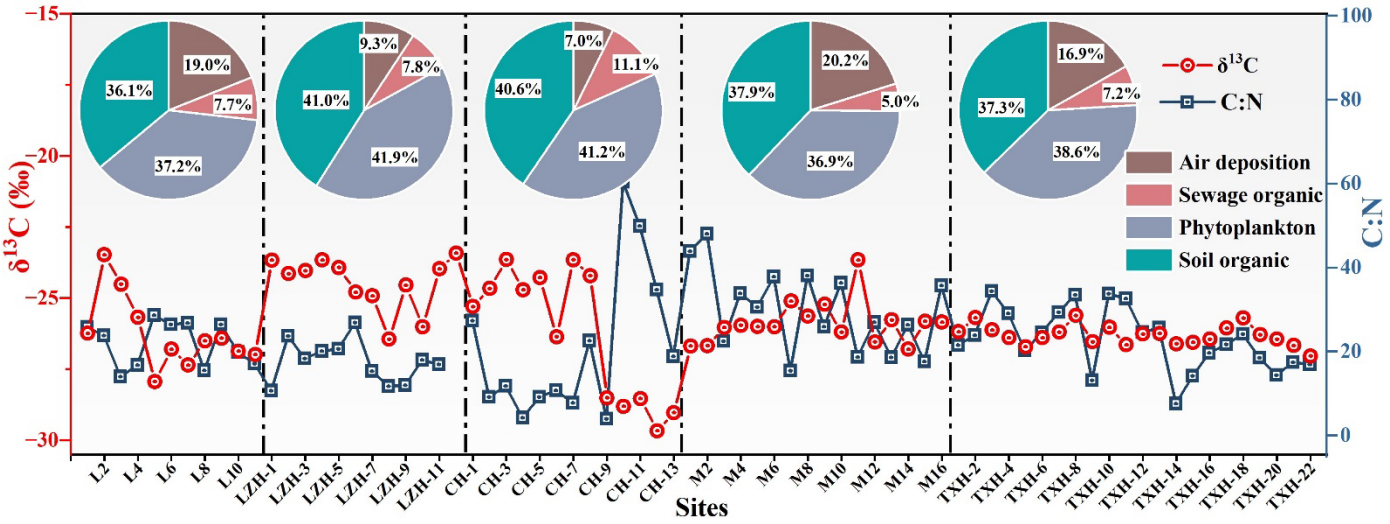

Fig 3. $\delta^{13}C$, C/N ratio values, and the percentage of organic matter source across the different lake sediments.

3.3 Mechanistic pathways controlling the PAHs fractionation

Driving forces behind the fractionation of PAHs in sediment were further explored by random forest (RF)

modelling and the Mantel test (Fig 4A-B). The OM source in atmospheric deposition significantly impacted the occurrence of BPAHs ($P < 0.01$), which suggests that rainfall could increase the bioavailability of PAHs in sediments by enhancing sediment resuspension, introducing dissolved organic carbon (DOC), and changing pH of overlying water (Marziali et al., 2017). Meanwhile, both LOC and atmospheric deposition were found to promote the occurrence of EPAHs in sediments, as supported by their positive correlations observed earlier (Fig S7 and S8). The high levels of EPAHs were thus attributed not only to direct inputs from anthropogenic pollution sources but also to enhanced LOC levels driven by physical disturbances within the lake sediment environment. ROC and OM derived from phytoplankton significantly influenced the NERs levels in sediment ($P < 0.01$), which was consistent with earlier findings (Fig S7 and S8). These results suggest that the OM inputs of phytoplankton and soil erosion could substantially increase the sedimentary ROC pool, thereby contributing notably to the increase in NERs.

We used SEM to investigate the causal pathways linking anthropogenic disturbances, hydrodynamic condition, OM sources, C-N fraction, and PAHs fraction (Fig 4C). For different PAH fractions, OM sources exhibited a significant direct effect on the C-N fraction (BPAHs: λ=0.353, P<0.01; EPAHs: λ=0.241, P<0.01; NERs: λ=0.156, P<0.05), and C-N fraction directly impacted three PAHs fraction (BPAHs: λ=0.110, P<0.05; EPAHs: λ=0.523, P<0.01; NERs: λ=0.407, P<0.01). These findings highlighted the moderating role of C-N fractions in the indirect effect of OM sources on PAH fractions. Significantly, anthropogenic disturbances directly exerted a positive influence on EPAHs (λ=0.365, P<0.001), and had direct negative effect on NERs (λ=-0.411, P<0.001). Potential explanations were that EPAHs were typically associated with recent anthropogenic emissions, whereas NERs represent aged and strongly bound PAHs fractions (Lu et al., 2024). The negative response of NERs may result from sediment disruption and enhanced desorption or transformation caused by anthropogenic disturbances. Meanwhile, anthropogenic disturbances directly

stimulated the abundance of C-N fraction (BPAHs: λ=-0.113, P<0.05; EPAHs: λ=0.712, P<0.01; NERs: λ=-0.783, P<0.01), thereby exerting an indirect influence on the distribution of PAH fractions. For EPAHs, anthropogenic disturbances had a significantly positive direct effect on OM source (λ = 0.538, P < 0.001) and hydrodynamic condition (λ = 0.508, P < 0.001), which can be attributed to the fact that enhanced sediment disturbances (increased DOC levels and active OM turnover) facilitate the mobilization and occurrence of EPAHs (Lan et al., 2018; Markiewicz et al., 2013). However, for NERs, anthropogenic disturbances exhibited significant negative effects on OM source (λ = -0.554, P < 0.001) and hydrodynamic condition (λ = -0.493, P < 0.001), likely due to the destabilization OM-PAH complexes and the desorption or transformation of NERs under higher disturbance conditions. Overall, sedimentary OM sources seem to exert primary control over the environmental retention of BPAHs, whereas C-N fractions, especially LOC and ROC, significantly influenced the occurrence of EPAHs and NERs. Further research is therefore warranted to clarify how C fraction regulated EPAHs and NERs formation.

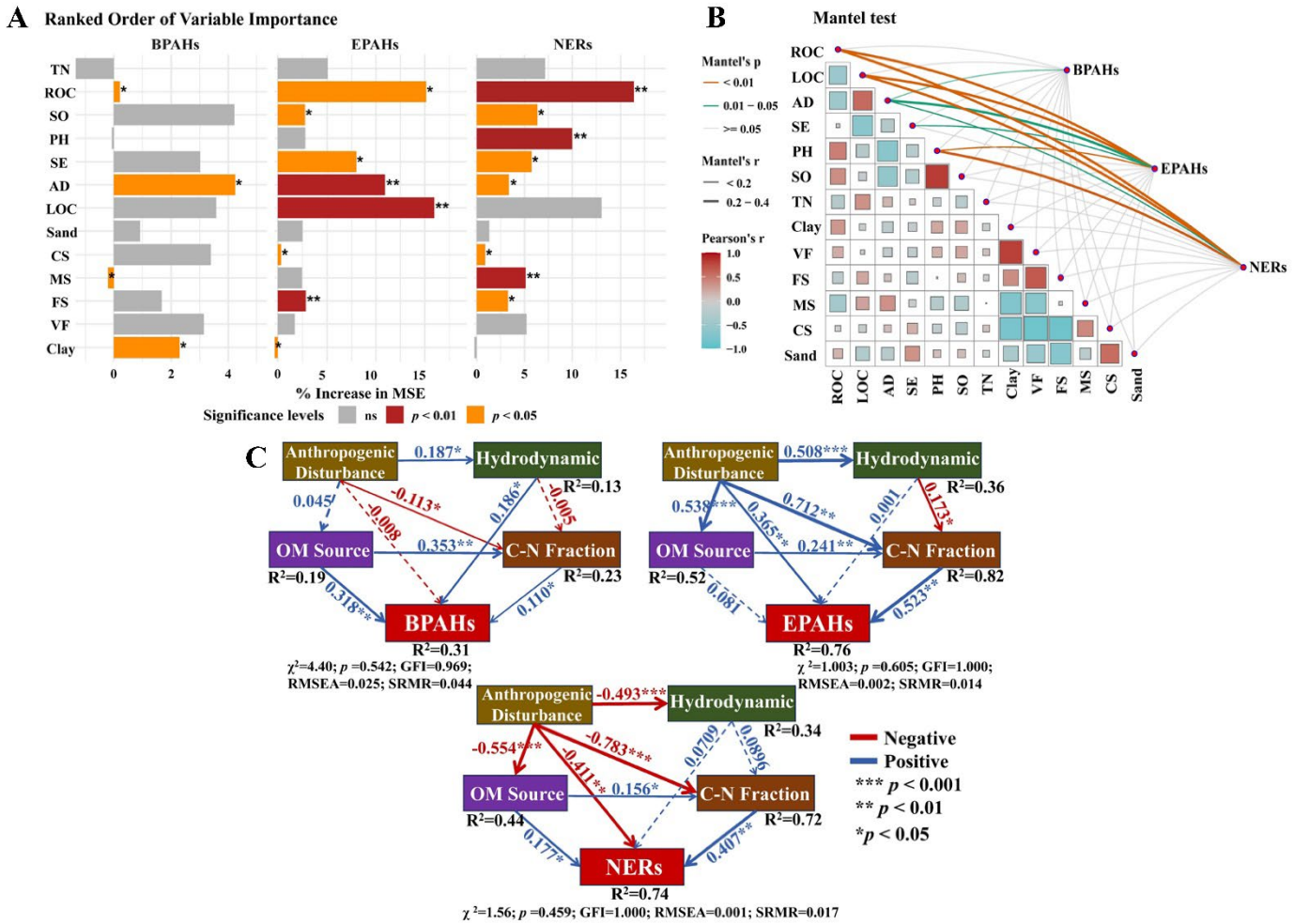

Fig 4. Mechanistic pathways controlling the PAHs fractionation. The importance of explanatory variables driving variation in three PAHs fraction (BPAHs, EPAHs, and NERs) using the random forest modelling analysis (A); Mantel test between sediment physicochemical properties and PAHs fraction (B). Structural equation model (SEM) revealing the effect of anthropogenic disturbances, hydrodynamic condition, OM sources (atmospheric deposition: AD, sewage organic input: SO, phytoplankton: PH, and soil erosion organic: SE), and C-N fraction (LOC, ROC, and TN) on the PAHs fraction (C). The standardized path coefficients (red arrow: negative and blue arrow: positive relationships) and significant ($P < 0.05$) and nonsignificant ($P > 0.05$) level were shown; R^2 demonstrated the proportion of variance explained. Anthropogenic disturbances for the different lake types.

3.4 Potential mechanisms for PAHs fractionation

3.4.1 The carbon cycling affects PAHs fractionation

Our modelled results showed that C fractions played a key regulatory role in determining the distribution of the three PAHs fractions, whereas other environmental variables, such as anthropogenic disturbances, hydrodynamic conditions, and OM sources, affected the patterns and concentrations of PAHs indirectly through modulating sedimentary C characteristics. Results showed that LOC was significantly positively correlated with extractable EPAHs ($R^2 = 0.479$, $r = 0.791$, $P < 0.0001$) but negatively correlated with NERs ($R^2 = 0.433$; $r = -0.658$, $P < 0.001$). In contrast, ROC exhibited a significant negative correlation with EPAHs (R^2=0.383, $r = -0.619$, $P < 0.001$) and a positive correlation with NERs ($R^2 = 0.440$, $r = 0.663$, $P < 0.0001$), highlighting the contrasting roles of LOC and ROC fractions in regulating the PAHs fractionation. Meanwhile, NERs were significantly positively correlated with sedimentary CSI and CUE, whereas EPAHs exhibited significant negative correlations with these parameters, as shown in Fig S9. These behaviors may be attributed to the role of stable and microbially efficient carbon pools in promoting the long-term sequestration of PAHs. More ROC (e.g., lignin, cellulose, and humin) tends to provide persistent sorption sites or physical entrapment within microporous, favoring the formation of NERs (Kästner et al., 2014; Lan et al., 2018). Higher CUE reflects the microbial assimilation of sediment carbon pools; however, increased microbial biomass and metabolic by-products may facilitate the formation of biogenic non-extractable residues (bioNER) by binding PAHs into biologically stabilized forms (Possberg et al., 2016). Additionally, LOC, as the most reactive and readily mineralizable fractions of the sedimentary OC pool, controlled the EPAH distributions in sediment probably due to the higher polarity, greater accessibility, and weaker sorption affinity of many LOC components (including low molecular weight organic acids and amino acids), as documented in previous studies (Hardison et al., 2013; Wu et al., 2012).

Generally, ROC/LOC has been used to present carbon transformation within biogeochemical cycles (Cheng et al., 2007; Lian et al., 2018). As shown in Fig 5, a significant negative correlation was observed

between ROC/LOC and EPAHs (R^2 = 0.524, P < 0.0001 for average; R^2 = 0.351, P < 0.001 for individual PAH), further indicating that lower ROC/LOC ratios (higher LOC levels) favor PAH extractability. Conversely, ROC/LOC exhibited a strong positive correlation with NERs (R^2 = 0.553 and 0.512, respectively), suggesting that higher proportions of ROC enhance PAH sequestration and promote the formation of NERs. However, the nonlinearity observed in the fitted power-law relationships between ROC/LOC and PAH fractions, highlighted the pivotal role of OC quality in modulating the environmental fate of PAHs. Higher LOC fraction in sediments was characterized by the high turnover rate, and the addition of exogenous OM can enhance the decomposition of sedimentary OM by approximately 50 % through this priming effect (Feng et al., 2011; Liu et al., 2023b; Lu et al., 2023). Accordingly, higher levels of LOC in lake sediments, particularly those under stronger anthropogenic influence, may further accelerate the accumulation of EPAHs, resulting in nonlinearity of the relationship. Meanwhile, log Kow of PAHs exhibited a positive relationship with the proportion of EPAHs and a negative relationship with NERs under high LOC conditions (Fig 5c-d), in agreement with the trends previously reported in Fig 2. Higher hydrophobicity (higher log Kow) promoted PAH partitioning into nonpolar extraction phases and enhanced desorption from sediment OM, thereby increasing the proportion of EPAHs (Liu et al., 2023c). EPAHs may primarily occupy the surface sorption sites of sedimentary OM associated with lower binding energies and relatively fast adsorption process (Heister et al., 2013; Lu et al., 2024). Conversely, higher hydrophobic PAHs were less able to penetrate sedimentary microporous structures or bind to high-energy sorption sites (humic acid and lipid fractions) (Northcott and Jones, 2001), resulting in a negative correlation between log Kow and NERs proportion. As previous studies reported, the formation of NERs was mainly driven by the sorption, physical entrapment, covalent and irreversibly bound, and biogenic NER (Kästner et al., 2014; Schäffer et al., 2018). It is therefore important to further elucidate the underlying mechanistic relationship between molecular descriptors of different PAH congeners and the average

percentage of non-extractable and extractable fraction in sediment.

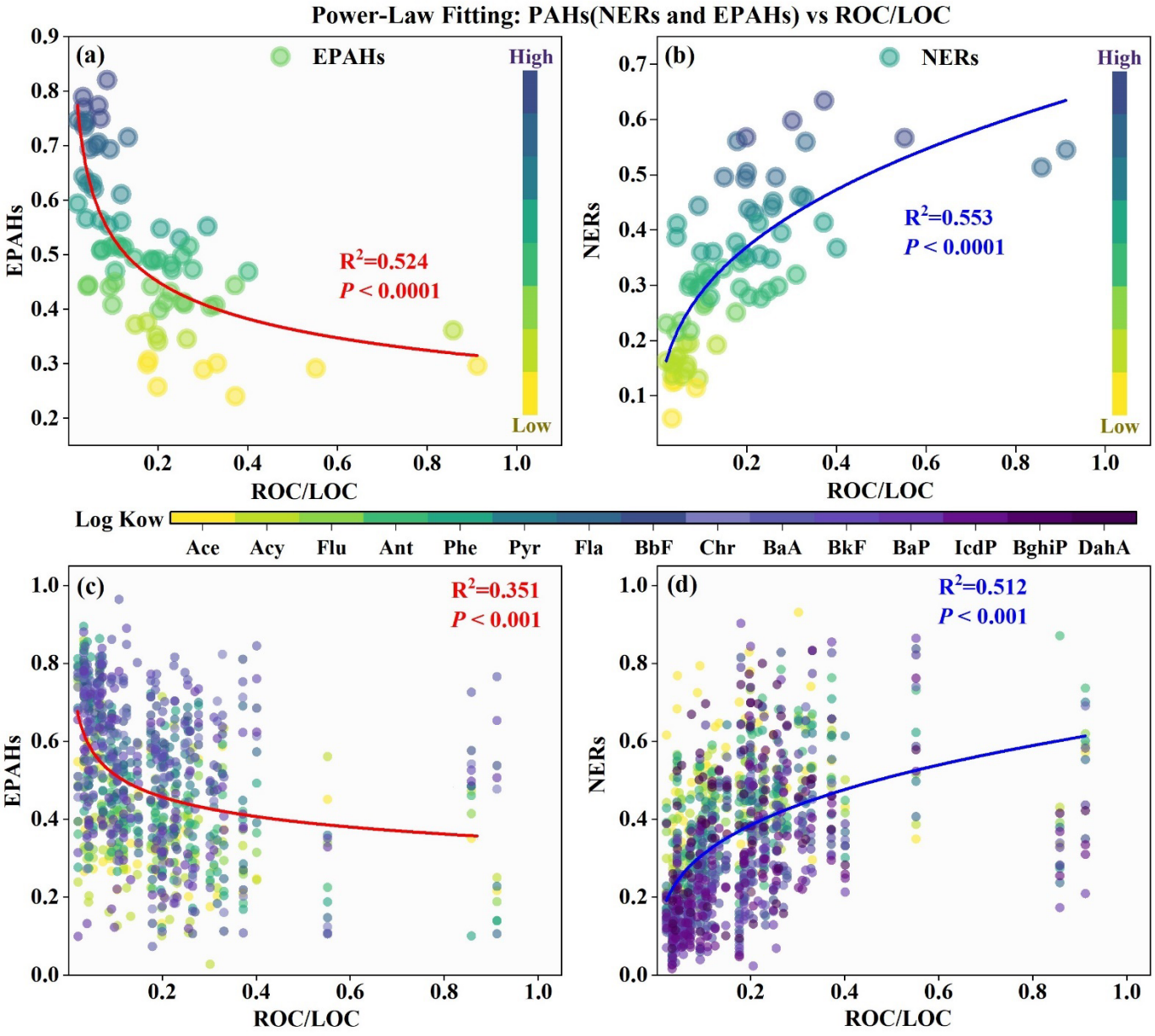

Fig 5. Power-law relationships between the proportion of PAHs (EPAHs and NERs) and ROC/LOC in sediments. (a, b): Fitted curves showing the average proportion of EPAHs and NERs across all sediment samples; (c, d) Corresponding relationships based on individual PAH congeners.

3.4.2 QSAR model

As part of this study we developed QSAR models based on machine learning (RF and PLS algorithm) between many molecular descriptors of individual PAH and the average percentage of NERs and EPAHs. As

shown in Fig S10, the RF algorithm had a better fit over the PLS algorithm in terms of both R^2 and RMSE, indicating better robustness and prediction ability. Results showed that the critical descriptors influencing the NERs formation were μ, α, qC^+, E, and E_{SCF}, whereas μ, CV, E_{gap}, S, and qC significantly influenced the EPAHs accumulation. Stronger molecular polarity (μ and α) controlled the binding ability of NERs with sediment matrices. The interaction potential (qC^+) represented more electrophilic sites and enhanced the electrophilicity toward sediment matrices by electrostatic attraction, hydrogen bonding, and π–π stacking, thereby promoting the accumulation of NERs (Anae et al., 2021; Barriuso et al., 2008). In contrast, EPAHs were more predominantly associated with descriptors indicating molecular reactivity and mobility. High E_{gap} is generally characterized by lower LUMO energy and higher HOMO energy, and EPAH compounds with higher E_{gap} (stable and low reactive) may be accumulated in sediment (Li et al., 2024). Meanwhile, qC enhanced the EPAHs binding with positively polarized sediment sites, and higher CV increased the van der Waals interactions within PAH and sediment OM (Gu et al., 2021; Niu and Gang, 2004). High entropy made ΔG_{ads} more negative and thus favored EPAHs accumulation in sediment (Mehmeti and Sadiku, 2022). In summary, the formation of NERs was primarily dictated by molecular polarity (μ, α) and electrophilic potential (qC^+) based on the electrostatic attraction, hydrogen bonding, and π–π stacking, whereas EPAHs accumulation was driven by molecular reactivity and mobility based on high Egap, increased entropy, and van der Waals interactions.

3.5 Implication for environmental risk assessment

In this section, BPAHs and EPAHs were directly compared to support the development of more accurate decision making in environmental risk assessment frameworks. For rural-type lakes, the calculated carcinogenic risks for both children and adults based on EPAHs were 5.34 and 4.78 times in LZH, 3.27 and

3.35 times in CH compared to those based on BPAHs (in Fig S11 and S12), respectively. However, the 50% ILRs for both children and adults derived from EPAHs and BPAHs indicated that the associated carcinogenic risks remain within acceptable limits. In contrast, urban lakes exhibited the clear carcinogenic risk when EPAHs were used in the calculations. The EPAHs- ILR distribution suggested that 2.40 % of children and 2.82 % of adults in LY, 7.48% of children and 6.72 % of adults in MS, 2.18% of children and 2.20 % of adults in LZH exceeding the acceptable threshold, respectively. By comparison, the lower proportions exceeding acceptable levels were 0.76 % of children and 0.70 % of adults in LY; 1.40% of children and 1.10 % of adults in MS; 0.58% of children and 0.46 % of adults in LZH, using the BPAHs calculated ILR distribution (see Fig S13-15). This reveals significant discrepancies between the two approaches. BPAHs appeared to yield a more accurate characterization of sedimentary carcinogenic hazard. We therefore recommend that bioavailability considerations were integrated into both PAH-based risk calculations and subsequent sediment management strategies to achieve the site-specific evaluation of carcinogenic potential. The formation of NERs has been shown to be primarily controlled through physicochemical sequestration and ester bonding (Guo et al., 2025b). Given that NERs can be easily remobilized, their substantial accumulation highlights a latent, long-term risk posed by PAHs to sediment ecosystems. Overall, this study highlighted the environmental fate of PAHs and the crucial role of BPAHs and the reversible nature of NERs in sediment. Further studies should be performed understanding environmental risk of the three formations of PAHs.

4. Conclusion

In summary, our study explored the accumulation mechanisms of PAHs in sediment by considering factors such as the anthropogenic disturbances, hydrodynamic conditions, OM sources, and SOC fractions. Importantly, anthropogenic emissions appeared to directly control the EPAHs occurrence in sediment, while

concurrently inhibiting the formation of NERs. Meanwhile, the environmental retention of BPAHs was associated with sedimentary OM sources, while SOC fractions significantly influenced the occurrence of EPAHs and NERs, especially LOC and ROC. Higher levels of LOC in lake sediments, especially in areas subject to stronger anthropogenic disturbances, may further enhance the accumulation of EPAHs, while higher proportions of ROC may promote the formation of NERs in sediment. We demonstrated that the log Kow of PAHs was positive correlated with the proportion of EPAHs, but negatively associated with NERs under high LOC conditions, which was related to the mechanistic relationship between molecular descriptors of different PAH congeners and the average proportion of NERs and EPAHs in sediment. Results of QSAR modelling further demonstrated that formation of NERs depended on the electrostatic attraction, hydrogen bonding, and π–π stacking, and was primarily influenced by molecular polarity (μ, α) and electrophilic potential (qC^+). However, EPAHs accumulation was mainly controlled by molecular reactivity and mobility due to high Egap, increased entropy, and van der Waals interactions. Finally, this study underscored the environmental fate of PAHs and emphasized the critical roles of BPAHs and reversible NERs in sedimentary systems.

Acknowledgement

The research was supported by the National Key Research and Development Program of China (2023YFC3709803); the National Natural Science Foundation of China (No. 42377235); the Fundamental Research Funds for the Central Universities, China University of Geosciences (Wuhan) (No. G1323523063; No. G1323524009); Weijie Liu acknowledges financial supports from the China Scholarship Council (No.202406410108).

References

Anae J, Ahmad N, Kumar V, Thakur VK, Gutierrez T, Yang XJ, et al. Recent advances in biochar

433 engineering for soil contaminated with complex chemical mixtures: Remediation strategies and future
434 perspectives. Science of the Total Environment 2021; 767.
435 Arzayus KM, Canuel EA. Organic matter degradation in sediments of the York River estuary: Effects of
436 biological vs. physical mixing. Geochimica Et Cosmochimica Acta 2005; 69: 455-464.
437 Bábek O, Kielar O, Lend'áková Z, Mandlíková K, Sedlácek J, Tolaszová J. Reservoir deltas and their role in
438 pollutant distribution in valley-type dam reservoirs: Les Kralovstvi Dam, Elbe River, Czech Republic.
439 Catena 2020; 184.
440 Barriuso E, Benoit P, Dubus IG. Formation of pesticide nonextractable (bound) residues in soil: Magnitude,
441 controlling factors and reversibility. Environmental Science & Technology 2008; 42: 1845-1854.
442 Cao R, Sun Y, Sun S, Sun XL, Meng FY, Xia YY, et al. Organic micropollutants in surface water across
443 China: Occurrence and ecological risk. Water Research 2025; 281.
444 Cheng C, Hu TP, Liu WJ, Mao Y, Shi MM, Xu A, et al. Modern lake sedimentary record of PAHs and OCPs
445 in a typical karst wetland, south China: Response to human activities and environmental changes.
446 Environmental Pollution 2021; 291.
447 Cheng L, Leavitt SW, Kimball BA, Pinter PJ, Ottmane MJ, Matthias A, et al. Dynamics of labile and
448 recalcitrant soil carbon pools in a sorghum free-air CO2 enrichment (FACE) agroecosystem. Soil
449 Biology & Biochemistry 2007; 39: 2250-2263.
450 Dodla SK, Wang JJ, DeLaune RD. Characterization of labile organic carbon in coastal wetland soils of the
451 Mississippi River deltaic plain: Relationships to carbon functionalities. Science of the Total
452 Environment 2012; 435: 151-158.
453 Dong L, Qi XR, Lin L, Zhao KF, Yin GC, Zhao LY, et al. Characteristics, sources, and concentration
454 prediction of endocrine disruptors in a large reservoir driven by hydrological rhythms: A case study of

the Danjiangkou Reservoir. Journal of Hazardous Materials 2025; 484.

Eltijani A, Molnár D, Makó L, Geiger J, Sümegi P. Application of Parameterized Grain-Size Endmember Modeling in the Study of Quaternary Oxbow Lake Sedimentation: A Case Study of Tovises Bed Sediments in the Eastern Great Hungarian Plain. Quaternary 2022; 5.

Feng WT, Schaefer DA, Zou XM, Zhang M. Shifting sources of soil labile organic carbon after termination of plant carbon inputs in a subtropical moist forest of southwest China. Ecological Research 2011; 26: 437-444.

Gevao B, Semple KT, Jones KC. Bound pesticide residues in soils: a review. Environmental Pollution 2000; 108: 3-14.

Gholami S, Behnami A, Arani MH, Kalantary RR. Impact of humic substances on the bioremediation of polycyclic aromatic hydrocarbons in contaminated soils and sediments: A review. Environmental Chemistry Letters 2024; 22: 889-918.

Gómez-Avila C, Rao B, Hussain T, Zhou HY, Pitt R, Colvin M, et al. Particle size-based evaluation of stormwater control measures in reducing solids, polycyclic aromatic hydrocarbons (PAHs) and polychlorinated biphenyls (PCBs). Water Research 2025; 277.

Gu LM, Zhu TY, Chen M. Modeling polyurethane foam (PUF)-air partition coefficients for persistent organic pollutants using linear and non-linear chemometric methods. Journal of Environmental Chemical Engineering 2021; 9.

Guo ML, Yu MX, Wang X, Xiao ND, Huguet A, Zhang YL, et al. Deciphering the link between particulate organic matter molecular composition and lake eutrophication by FT-ICR MS analysis. Water Research 2025a; 272.

Guo XR, Wu X, Cao SQ, Wang LH, Kong DY, Wang YF, et al. Fate and Persistence of Bisphenol AF

(BPAF) in Agricultural Soils: Role of Nonextractable Residues. Environmental Science & Technology 2025b; 59: 10488-10497.

Hardison AK, Canuel EA, Anderson IC, Tobias CR, Veuger B, Waters MN. Microphytobenthos and benthic macroalgae determine sediment organic matter composition in shallow photic sediments. Biogeosciences 2013; 10: 5571-5588.

Hasan O, Smrkulj N, Miko S, Brunovic D, Ilijanic N, Miko MS. Integrated Reconstruction of Late Quaternary Geomorphology and Sediment Dynamics of Prokljan Lake and Krka River Estuary, Croatia. Remote Sensing 2023; 15.

Heister K, Pols S, Loch JPG, Bosma TNP. Desorption behaviour of polycyclic aromatic hydrocarbons after long-term storage of two harbour sludges from the port of Rotterdam, The Netherlands. Journal of Soils and Sediments 2013; 13: 1113-1122.

Ji KY, Ouyang W, Lin CY, He MC, Liu XT. Eco-hydrological processes regulate lake riparian soil organic matter under dryness stress. Water Research 2024; 260.

Kästner M, Nowak KM, Miltner A, Trapp S, Schäffer A. Classification and Modelling of Nonextractable Residue (NER) Formation of Xenobiotics in Soil - A Synthesis. Critical Reviews in Environmental Science and Technology 2014; 44: 2107-2171.

Khan MYA. Evaluating the Spatial Variations in Bed Sediment and Their Depositional Environments Using Particle-Size Analysis of Wadi Fatima, Saudi Arabia. Water 2024; 16.

Lan JC, Sun YC, Yuan DX. Transport of polycyclic aromatic hydrocarbons in a highly vulnerable karst underground river system of southwest China. Environmental Science and Pollution Research 2018; 25: 34519-34530.

Li GQ, Zhang YF, Li CA. Lake Evolution and Its Response to Urban Expansion in Wuhan City in the Last

Hundred Years Based on Historical Maps and Remote Sensing Images. Remote Sensing 2025; 17.

Li SY, Zhang SN, Xu JQ, Guo RX, Allam AA, Rady A, et al. Photodegradation of polycyclic aromatic hydrocarbons on soil surface: Kinetics and quantitative structure-activity relationship (QSAR) model development. Environmental Pollution 2024; 345.

Lian ZL, Jiang ZJ, Huang XP, Liu SL, Zhang JP, Wu YC. Labile and recalcitrant sediment organic carbon pools in the Pearl River Estuary, southern China. Science of the Total Environment 2018; 640: 1302-1311.

Liao JH, Wang XY, Wang HJ, Hou MC, Zhou SZ, Shi ZM, et al. Geographical impact on the distribution of polycyclic aromatic hydrocarbons (PAHs) in hilly terrain topsoil: A case study at Chongqing, SW, China. Journal of Hazardous Materials 2025; 487.

Liu J, Wang YF, Jiang BQ, Wang LH, Chen JQ, Guo HY, et al. Degradation, Metabolism, and Bound-Residue Formation and Release of Tetrabromobisphenol A in Soil during Sequential Anoxic-Oxic Incubation. Environmental Science & Technology 2013; 47: 8348-8354.

Liu JB, Zhang C, Jia HZ, Lichtfouse E, Sharma VK. Abiotic transformation of polycyclic aromatic hydrocarbons via interaction with soil components: A systematic review. Critical Reviews in Environmental Science and Technology 2023a; 53: 676-699.

Liu LX, Kang Y, Hu Z, Wu HM, Guo ZZ, Zhang J. Evaluation of individual and combined effects of microplastics and naphthalene on aquatic sediment: Disturbance of carbon and microbial dynamics. Journal of Hazardous Materials 2025; 495.

Liu XL, Dong ZW, Baccolo G, Gao WH, Li QL, Wei T, et al. Distribution, composition and risk assessment of PAHs and PCBs in cryospheric watersheds of the eastern Tibetan Plateau. Science of the Total Environment 2023b; 890.

Liu Y, He Y, Han B, Liu H, Tao S, Liu W. Sewage discharge and organic matter affect the partitioning behaviors of different polycyclic aromatic hydrocarbons in a river surface sediment-pore water system. Journal of Hazardous Materials 2023c; 446: 130757.

Lu ZY, Tian WJ, Chu ML, Zhang SR, Zhao J, Liu BK, et al. A novel and thorough research into desorption behavior of PAHs from sediments to seawater: Aging process, thermodynamics, kinetics, influencing factors. Chemical Engineering Journal 2024; 480.

Lu ZY, Xiao K, Wang FF, Wang Y, Yu QB, Chen NW. Salt marsh invasion reduces recalcitrant organic carbon pool while increases lateral export of dissolved inorganic carbon in a subtropical mangrove wetland. Geoderma 2023; 437.

Luo J, Huang GB, Wang M, Zhang YN, Liu ZX, Zhang Q, et al. Composition characteristics, source analysis and risk assessment of PAHs in surface waters of Lipu. Journal of Hazardous Materials 2025; 490.

Ma NJ, Tong L, Li YQ, Yang C, Tan Q, He J. Distribution of antibiotics in lake water-groundwater-Sediment system in Chenhu Lake area. Environmental Research 2022; 204.

Ma WW, Li G, Wu JH, Xu GR, Wu JQ. Response of soil labile organic carbon fractions and carbon-cycle enzyme activities to vegetation degradation in a wet meadow on the Qinghai-Tibet Plateau. Geoderma 2020; 377.

Ma YF, Chen ML, Yi P, Guo RX, Ji R, Chen JQ, et al. Transformation and environmental fate of 6-OH-BDE-47 and 6-MeO-BDE-47 in oxic and anoxic sediments. Journal of Hazardous Materials 2025; 483.

Maletic SP, Beljin JM, Roncevic SD, Grgic MG, Dalmacija BD. State of the art and future challenges for polycyclic aromatic hydrocarbons is sediments: sources, fate, bioavailability and remediation techniques. Journal of Hazardous Materials 2019; 365: 467-482.

Markiewicz M, Jungnickel C, Arp HPH. Ionic Liquid Assisted Dissolution of Dissolved Organic Matter and

543 PAHs from Soil Below the Critical Micelle Concentration. Environmental Science & Technology 2013;
544 47: 6951-6958.
545 Marquès M, Mari M, Sierra J, Nadal M, Domingo JL. Solar radiation as a swift pathway for PAH
546 photodegradation: A field study. Science of the Total Environment 2017; 581: 530-540.
547 Marziali L, Tartari G, Salerno F, Valsecchi L, Bravi C, Lorenzi E, et al. Climate Change Impacts on
548 Sediment Quality of Subalpine Reservoirs: Implications on Management. Water 2017; 9.
549 Mehmeti V, Sadiku M. A Comprehensive DFT Investigation of the Adsorption of Polycyclic Aromatic
550 Hydrocarbons onto Graphene. Computation 2022; 10.
551 Niu JF, Gang Y. Molecular structural characteristics governing biocatalytic oxidation of PAHs with
552 hemoglobin. Environmental Toxicology and Pharmacology 2004; 18: 39-45.
553 Niu JY, Jin G, Zhang L. Territorial spatial zoning based on suitability evaluation and its impact on ecosystem
554 services in Ezhou city. Journal of Geographical Sciences 2023; 33: 2278-2294.
555 Northcott GL, Jones KC. Partitioning, extractability, and formation of nonextractable PAH residues in soil.
556 1. Compound differences in aging and sequestration. Environmental Science & Technology 2001; 35:
557 1103-1110.
558 Possberg C, Schmidt B, Nowak K, Telscher M, Lagojda A, Schaeffer A. Quantitative Identification of
559 Biogenic Nonextractable Pesticide Residues in Soil by 14C-Analysis. Environmental Science &
560 Technology 2016; 50: 6415-6422.
561 Qin SB, Han E, Li XS, Liu WJ, Hu TP, Qi SH. Effects of nonextractable residual formation on the study of
562 historical PAH pollution and source contribution in a lake sediment core. Environmental Pollution
563 2025; 377.
564 Qin SB, Li XS, Han ER, Fan YH, Liu SH, Ding Y, et al. Strategies and mechanisms for improving the

565 detection accuracy of nonextractable residues of polycyclic aromatic hydrocarbons in soils. Science of
566 the Total Environment 2024; 943.
567 Qin SB, Qi SH, Li XS, Shi QY, Li H, Mou XX, et al. Magnetic poly(β-cyclodextrin) combined with
568 solubilizing agents for the rapid bioaccessibility measurement of polycyclic aromatic hydrocarbons in
569 soils. Environmental Pollution 2021; 291.
570 Schäffer A, Kästner M, Trapp S. A unified approach for including non-extractable residues (NER) of
571 chemicals and pesticides in the assessment of persistence. Environmental Sciences Europe 2018; 30.
572 Serrano O, Rozaimi M, Lavery PS, Smernik RJ. Organic chemistry insights for the exceptional soil carbon
573 storage of the seagrass Posidonia australis. Estuarine Coastal and Shelf Science 2020; 237.
574 Shi MM, Li R, Xu A, Su YW, Hu TP, Mao Y, et al. Huge quantities of microplastics are "hidden" in the
575 sediment of China's largest urban lake-Tangxun Lake. Environmental Pollution 2022; 307.
576 Sinsabaugh RL, Turner BL, Talbot JM, Waring BG, Powers JS, Kuske CR, et al. Stoichiometry of microbial
577 carbon use efficiency in soils. Ecological Monographs 2016; 86: 172-189.
578 Skic K, Boguta P, Klimkowicz-Pawlas A, Ukalska-Jaruga A, Baran A. Effect of sorption properties on the
579 content, ecotoxicity, and bioaccumulation of polycyclic aromatic hydrocarbons (PAHs) in bottom
580 sediments. Journal of Hazardous Materials 2023; 442.
581 Trevathan-Tackett SM, Macreadie PI, Sanderman J, Baldock J, Howes JM, Ralph PJ. A Global Assessment
582 of the Chemical Recalcitrance of Seagrass Tissues: Implications for Long-Term Carbon Sequestration.
583 Frontiers in Plant Science 2017; 8.
584 Wei R, Wei ST, Yao C, Chen WF, Yang LM, Ni JZ. Distribution and biodegradation of nonextractable
585 polycyclic aromatic hydrocarbons in particle-size aggregates of field-contaminated soils. Journal of
586 Soils and Sediments 2023; 23: 3748-3760.

Wei R, Yang MY, Yao C, Chen WF, Yang LM, Ni JZ. Characteristics and Biodegradation of Nonextractable Residues of Polycyclic Aromatic Hydrocarbons in Historically Polluted Soils. Water Air and Soil Pollution 2024; 235.

Wu FC, Xu LB, Sun YG, Liao HQ, Zhao XL, Guo JY. Exploring the relationship between polycyclic aromatic hydrocarbons and sedimentary organic carbon in three Chinese lakes. Journal of Soils and Sediments 2012; 12: 774-783.

Wu X, Sun FF, Cao SQ, Wang QL, Wang LH, Wang SF, et al. Maize (Zea mays L.) Plants Alter the Fate and Accumulate Nonextractable Residues of Sulfamethoxazole in Farmland Soil. Environmental Science & Technology 2024; 58: 9292-9302.

Xing XL, Liu WJ, Li P, Su YW, Li XY, Shi MM, et al. Insight into the effect mechanism of sedimentary record of polycyclic aromatic hydrocarbon: Isotopic evidence for lake organic matter deposition and regional development model. Environmental Research 2023; 239.

Ya M, Wu YL, Wang XH, Wei HC. Fine particles and pyrogenic carbon fractions regulate PAH partitioning and burial in a eutrophic shallow lake. Environmental Pollution 2022; 314.

Yun XM, Zhang LD, Wang WJ, Gu JQ, Wang YF, He YJ, et al. Composition, Release, and Transformation of Earthworm Tissue-Bound Residues of Tetrabromobisphenol A in Soil. Environmental Science & Technology 2024; 58: 2069-2077.

Zeng J, Wu RN, Peng TT, Li QG, Wang Q, Wu YC, et al. Low-temperature thermally enhanced bioremediation of polycyclic aromatic hydrocarbon-contaminated soil: Effects on fate, toxicity and bacterial communities. Environmental Pollution 2023; 335.

Zhang SZ, Xing XL, Yu HK, Du MK, Zhang Y, Li P, et al. Fate of polycyclic aromatic hydrocarbon (PAHs) in urban lakes under hydrological connectivity: A multi-media mass balance approach☆.

609 Environmental Pollution 2025; 366.
610 Zhang Y, Shen J, Feng JM, Li XY, Liu HJ, Wang XZ. Composition, distribution, and source of organic
611 carbon in surface sediments of Erhai Lake, China. Science of the Total Environment 2023; 858.
612 Zhu XJ, Yang F, Li Z, Fang ML, Ma SP, Zhang T, et al. Substantial halogenated organic chemicals stored in
613 permafrost soils on the Tibetan Plateau. Nature Geoscience 2023; 16: 989-+.
614